NATIONAL ADVISORY COMMITTEE FOR AERONAUTICS

TECHNICAL NOTE 2668

EXPERIMENTAL INVESTIGATION OF A 90° CASCADE DIFFUSING BEND WITH AN AREA RATIO OF 1.45:1 AND WITH SEVERAL INLET BOUNDARY LAYERS

By Daniel Friedman and Willard R. Westphal

Langley Aeronautical Laboratory
Langley Field, Va.

Washington
April 1952

1L

NATIONAL ADVISORY COMMITTEE FOR AERONAUTICS

TECHNICAL NOTE 2668

EXPERIMENTAL INVESTIGATION OF A 90° CASCADE DIFFUSING BEND WITH AN AREA RATIO OF 1.45:1 AND WITH SEVERAL INLET BOUNDARY LAYERS

By Daniel Friedman and Willard R. Westphal

SUMMARY

An experimental investigation was conducted in order to determine the performance of a 90° cascade diffusing bend, with an area ratio of 1.45:1, a 19- by 19-inch inlet, and five inlet boundary layers, varying from an approximate over-all thickness of 1/4 inch and a shape parameter of 1.22 to an approximate over-all thickness of $6\frac{1}{2}$ inches and a shape parameter of 1.67. Tests were made at inlet Mach numbers up to 0.41 and at Reynolds numbers, based on the cascade airfoil chord of 4 inches, of from 330,000 to 950,000.

The diffuser effectiveness varied from about 0.74 for the tests with the thinnest inlet boundary layer to about 0.19 for the tests with the thickest inlet boundary layer. The total-pressure-loss coefficient for the tests with the thinnest inlet boundary layer was about 0.11 and increased to about 0.24 for the thickest inlet boundary layer.

The total-pressure-loss coefficient of the cascade diffusing bend, for the thick inlet boundary range, was found to be about equal to the coefficient obtained for a vaned bend without any diffusion. This result indicates that, when a duct configuration requires a vaned bend, a certain amount of diffusion can probably be obtained without an appreciable increase in the energy losses. In addition, when length is important, this configuration is much shorter than the usual diffuser-bend combination.

INTRODUCTION

The usual approach in the design of internal-flow systems which require efficient diffusion and turning of the flow is to select a small-included-angle diffuser followed by a vaned bend. Since the losses in the bend depend upon the velocity of the flow entering the bend, as much diffusion as is feasible is accomplished in the diffuser before the flow

enters the bend. In wind-tunnel diffusers, aircraft duct systems, and similar applications, however, available space limits the length of the diffuser. For such applications, the achievement of efficient diffusion and turning becomes difficult.

If very short diffusers are necessary, boundary-layer control can be used to improve the performance of the diffuser. This type of configuration, however, requires auxiliary equipment. Some work has been done on diffusing and turning the flow in a cascade. Cascade studies of compressor blades in porous-wall two-dimensional cascade tunnels (reference 1) show that efficient turning can be obtained for turning angles up to 30°. Reference 2 shows that, with no diffusion, turning angles as high as 110° have been obtained without incurring prohibitive losses in total pressure. On the basis of these results, the use of a cascade-type diffusing bend seemed worthy of consideration, even though no information was available on the performance of a 90° diffusing bend and even though the presence of an appreciable inlet boundary layer was expected to increase the total-pressure losses and reduce the static-pressure rise. The prospect of obtaining some diffusion in a right-angled bend was attractive enough to warrant study and an investigation of the performance of a cascade diffusing bend was undertaken. The configuration selected for this investigation was a right-angle bend with a 19- by 19-inch inlet and an area ratio of 1.45:1. A cascade of airfoils was located at the plane of intersection of the inlet and exit ducts.

In order to determine the effect of inlet-boundary-layer shape and thickness on the performance of the cascade bend, five different inlet boundary layers were used in the investigation. The thinnest inlet boundary layer approximates the boundary layer that would be expected in a duct behind a wing or nose inlet without any diffusion. The thickest inlet boundary layer is similar to the boundary layer that would be expected at the downstream end of a simple rectangular diffuser in which the flow was on the verge of separating in the corners. Tests were made at Mach numbers up to 0.41. The Reynolds number, based on airfoil chord, varied from 330,000 to 950,000, which is well above the critical Reynolds number for cascade airfoils. (See reference 1.)

SYMBOLS

A	total cross-sectional area at station, square inches
H	two-dimensional boundary-layer-shape parameter for incompressible flow (δ^*/θ)
$\bar{H}$	three-dimensional boundary-layer-shape parameter for incompressible flow (Δ^*/ϕ)

h local total pressure, pounds per square foot

p local static pressure, pounds per square foot

q_c local impact pressure, pounds per square foot $(h - p)$

$$\bar{q}_c = \frac{\int_0^A uq_c \, dA}{\int_0^A u \, dA}$$

U maximum stream velocity at section under consideration, feet per second

u local velocity within the boundary layer, feet per second

V theoretical velocity upstream of airfoils, feet per second

v theoretical local velocity on airfoil surface, feet per second

Δ^* three-dimensional boundary-layer displacement area, square inches

Δ' area of boundary layer, measured from wall, beyond which a negligible contribution is made to the values of the Δ^* and ϕ integrals, square inches

δ boundary-layer thickness $\left(\text{at } \frac{u}{U} = 0.95\right)$, inches

δ^* boundary-layer displacement thickness, inches

θ boundary-layer momentum thickness, inches

ρ local density, slugs per cubic foot

ϕ three-dimensional boundary-layer momentum area, square inches

Subscripts are used to denote the station (fig. 1) at which the quantity was measured, and a bar above the symbol is used to denote the mean value at the station under consideration.

APPARATUS AND METHOD

Before entering the diffusing bend, the air stream passed from a 54-inch-diameter duct into two convergent sections with an over-all contraction ratio of 6.6 to 1. The first convergent section made a transition from the 54-inch diameter to a 22-inch square and the second accomplished the remaining convergence to a 19-inch square. When necessary, boundary-layer-control devices were inserted downstream of the convergent sections and the diffusing bend. A parallel-sided rectangular duct 10 feet, 9 inches long was attached to the exit of the diffusing bend. A sketch of the test setup is shown in figure 1.

Cascade diffusing bend.- The diffusing bend investigated consisted of two rectangular ducts, one 19 by 19 inches and the other 19 by 27.55 inches, at right angles to each other, with the cascade of airfoils at their intersection. For this duct arrangement, the area ratio was 1.45:1 and the air-inlet angle was 55.4°. A photograph of the diffusing bend, with the airfoils partly removed to show their location, is shown in figure 2. A sketch of the cascade is presented in figure 3.

The product of solidity and lift coefficient, based on the velocity of the entering air, was computed from the geometry of the bend and a momentum analysis of the flow to be 1.48. On the basis of previous experience a solidity of 2.0 was selected. At this solidity, which was obtained by using a cascade of 15 equally spaced airfoils, the required blade lift coefficient is approximately 0.75, a value readily obtained in a cascade of this type. The desired turning was obtained by using airfoils having a mean-line curvature of 105.5° (an induced angle of 5° and a deviation angle at the trailing edge of 10.5° being assumed). The cascade airfoil profiles are formed from two circular arcs of different radii and centers to give 4-inch-chord airfoils of approximately 10-percent thickness. The resulting airfoil profile is shown in figure 4. The corners of the bend had the same radii as the corresponding surfaces of the airfoils. (See fig. 3.)

The flow pattern for this cascade was determined by the use of the wire-mesh flow-plotting device described in reference 3 in order to check the peak velocity and rate of diffusion on the upper surface. A photograph of the flow pattern derived by the use of this device is shown in figure 5, and the airfoil pressure distribution thus determined is presented in figure 6. The estimated critical Mach number, based on this pressure distribution, is 0.67.

Boundary-layer-control devices.- In order to determine the effect of inlet boundary layer on the performance of the cascade diffusing bend, five different inlet boundary layers with varying thickness and

shape parameters were used in this investigation. This variation in boundary-layer thickness and shape parameter was obtained by using boundary-layer screens, boundary-layer fences, and a 5-foot-long square duct. The boundary-layer screens consisted of several layers of brass hardware cloth fastened to a wooden frame. Square holes of different size were cut into the center of each layer. The boundary-layer fences consisted of a number of $\frac{1}{4}$-inch steel rods, spaced 1 inch apart, which could be projected into the air stream any desired amount. For some tests, a 5-foot section of duct was placed between the boundary-layer control devices and the diffusing bend inlet. Table I gives the dimensions of the screens and the rod settings used in this investigation. The boundary-layer parameters for each test condition are presented in table II.

The two-dimensional boundary-layer parameters were calculated from the standard equations given in reference 4 and elsewhere. The three-dimensional parameters were calculated from the following equations:

$$\Delta^* = \frac{\rho U\Delta' - \rho\int_0^{\Delta'} u\, dA}{\rho U}$$

$$\phi = \frac{\rho u\int_0^{\Delta'} u\, dA - \rho\int_0^{\Delta'} u^2 dA}{\rho U^2}$$

For the thinnest inlet boundary layer, no boundary-layer-control devices were used. This boundary layer approximates one that would be expected in a duct behind a wing or nose inlet without any diffusion. Figure 7 shows the screen and fence setting used for the thickest boundary-layer configuration. This boundary layer is similar to the boundary layer that would be expected downstream of a simple rectangular diffuser in which the flow was on the verge of separating in the corners.

Instrumentation

The flow properties were measured at the four stations shown in figure 1. The mass flow was determined from static and total-pressure

measurements made at station I from a calibration chart prepared by placing a venturi meter in series with the large transition section. The flow pattern of the air entering the cascade was measured at station II. At this station, which is $15\frac{1}{2}$ inches upstream of the nearest cascade airfoil, four fixed total-pressure rakes were installed in the corners and four adjustable pitot-static survey tubes were mounted in the center of each of the four sides. Eight static orifices, two on each wall, were used to measure the wall static pressure at this station. The instrumentation at station III, which was $12\frac{1}{2}$ inches downstream of the nearest airfoil, was the same as at station II. Only the static pressure was measured at station IV.

Experimental Procedure

For a given boundary-layer screen and fence setting, flow surveys were made at stations I and II over a range of mass flows. The rakes were then moved to station III and a complete set of data was taken at stations I, III, and IV. The same procedure was used for the other inlet-boundary-layer tests.

RESULTS AND DISCUSSION

Velocity Distribution

In this investigation, in which air flowed through a 90° bend with diffusion, the boundary layer was expected to be a dominant factor. Accordingly, detailed pressure surveys were made ahead of and behind the cascade of airfoils.

Inlet flow.- Figure 8 presents a pictorial representation of the inlet-velocity distribution for a thin and a thick inlet-boundary-layer configuration. Since the flow was symmetrical, the flow for only one quadrant was presented. For the same boundary-layer fence and screen setting, no change in the flow pattern was observed with a variation of mass flow.

The inlet boundary layers were quite uniform and no velocity irregularities were observed. The boundary-layer parameters describing the inlet flows are listed in table II. For purposes of comparison, the inlet boundary layer for fully developed turbulent pipe flow is of interest. The one-seventh-power velocity distribution for turbulent pipe flow gives a two-dimensional shape parameter of 1.29 and a two-dimensional momentum thickness θ of 0.92 inch for a 19-inch-diameter pipe. The data of

table II show that configuration 5 has a more adverse inlet boundary-layer condition than that for fully developed turbulent pipe flow.

Table II shows that the boundary-layer shape parameter increased with increasing boundary-layer thickness. This combination of increasing thickness and shape parameters, both of which should have an adverse effect on performance, was imposed in order to get boundary layers similar to those obtained downstream of a symmetrical rectangular diffuser.

Exit flow.- Figure 9 gives a pictorial representation of the exit velocity distribution for the same flow conditions as figure 8 and was constructed in the same manner. Since the flow was symmetrical about the horizontal center line, only the top half of the flow pattern was presented.

A very slow random variation of the exit velocity profile was observed during the tests. The velocity increased in one region and decreased in another. The profiles shown are the averages of the data obtained. The maximum variation, due to unsteady flow, amounted to about ±5 percent of the mean local value. This phenomenon was more noticeable for the thicker inlet boundary layers and is similar to the phenomena observed in wide angle diffusers. It is probably due to an alternating or intermittent separation or flow-reversal condition.

Figure 9 shows that, even for a relatively thin inlet boundary layer (configuration 2), the velocity is less at the inside corner than at the outside corner. This phenomenon is associated with the flow of the boundary layer from the other walls into the inside corner and separation near the inside corner. The flow conditions might have been better if the spacing between the inside corner and the first airfoil had been reduced to bring about a reduction in the pressure gradient on the inside wall.

The exit boundary-layer parameters are listed in table II. No two-dimensional boundary-layer parameters are presented, since the lack of symmetry would require far too many values to cover the flow picture.

Performance

Inasmuch as the shape and thickness of the inlet boundary layer strongly affects the inlet and exit velocity distributions, these conditions can also be expected to affect the performance of this cascade bend.

The variation of the performance parameters with inlet three-dimensional momentum area ϕ is shown in figure 10 for a mean inlet

Mach number of 0.30 (mass-flow constant ±10 percent). The three-dimensional momentum area was used because it takes into account the variation of boundary-layer shape and thickness around the perimeter of the duct. It should be remembered that the inlet boundary layers are measured at a station that is $15\frac{1}{2}$ inches ahead of the nearest airfoil. The thinner boundary layers change appreciably in this distance. For example, the thinnest two-dimensional boundary layer measured on the wall will thicken by a factor of about 2.5 before reaching the center blade.

Since the inlet and exit data were taken during different tests, the use of faired curves was necessary in order to get corresponding inlet and exit data. As a result, data points could not be shown on the performance curves.

The slow random variation in flow pattern previously discussed is evident in the data of figure 10. The maximum and minimum values obtained for each parameter are shown in figure 10. The configurations for which data were obtained are shown by vertical dash lines. Unless otherwise stated, all the parameters discussed are average values.

Total-pressure-loss coefficient.- The total-pressure-loss coefficient is a measure of the amount of available energy which is dissipated in friction, separation, and similar losses. It is defined as the loss in total pressure divided by the entering impact pressure.

The data in figure 10 show that the total-pressure-loss coefficient increased from a value of 0.11 at an inlet ϕ of 2 to a value of 0.24 at an inlet ϕ of 71. This large increase in loss coefficient with increasing inlet momentum area shows that the boundary-layer effects have a large adverse influence on the performance of the cascade diffusing bend, as had been anticipated. In the light of this information, much better performance would be expected in a cascade diffusing bend in which the boundary-layer effects were completely eliminated.

In order to determine the magnitude of the improvement in performance that could be obtained with boundary-layer control, the performance of the diffusing bend was compared with the performance of a similar cascade tested in the Langley 5-inch cascade tunnel, where the boundary-layer effects are reduced to a negligible value by the use of

boundary-layer-control slots and porous walls. A comparison of the two cascades is given in the following table:

	Porous-wall cascade	Diffusing-bend configuration 1
Thickness distribution	NACA 65-series	Circular-arc surfaces
Mean line	Circular arc	Circular arc
Turning angle, design	75.0	90.0
Turning angle, measured	79.8	----
Area ratio	1.48	1.45
Solidity	2.10	2.0
Reynolds number	501,000	400,000 to 950,000
Total-pressure-loss coefficient	0.029	0.11

The results of these tests show that the total-pressure-loss coefficient obtained from the porous-wall cascade-tunnel tests was only about one-fourth of the value obtained for the cascade diffusing bend with the thinnest boundary layer investigated. This large difference in loss coefficient is obtained even though the pressure gradient measured in the porous-wall cascade was not radically different from that of the calculated pressure gradient for the cascade used in the diffusing bend (fig. 11). (For high solidity cascades, reference 3 shows good agreement between the calculated and experimental pressure distributions.) This difference in loss coefficient would seem to indicate that, for the configuration investigated, the total-pressure losses due to airfoil boundary layer are only a small part of the total losses and that the duct boundary-layer effects are predominant. It would seem likely, therefore, that a large improvement in performance could be obtained through the use of boundary-layer control.

Diffusion factor.- The diffusion factor is defined as the ratio of the actual drop in impact pressure between the stations under consideration to the theoretical drop calculated from the mean inlet conditions and the physical area ratio for an assumed uniform velocity distribution at the exit. Figure 10 shows the variation of this parameter with the inlet three-dimensional momentum area for a mean inlet Mach number 0.30.

The diffusion factor varies from a value of 0.95 at ϕ equal to 2 to a value of 0.56 at ϕ equal to 71.

Diffuser effectiveness.- The diffuser effectiveness is defined as the ratio of the actual static pressure rise between the stations under consideration to the theoretical ideal pressure rise calculated from the

mean inlet conditions and the physical area ratio for a uniform velocity distribution at the exit.

Figure 10 shows the variation of diffuser effectiveness with inlet three-dimensional momentum displacement area. This parameter varies from a value of 0.74 at an inlet ϕ of 2 to a value of 0.19 at a ϕ of 71.

For the porous-wall cascade-tunnel tests previously described, a diffuser effectiveness of 0.925 was obtained. This value of the diffuser effectiveness is much larger than the value of 0.742 obtained for the cascade diffusing bend with the thinnest boundary layer investigated. This large difference in diffuser effectiveness would seem to indicate that the wall boundary-layer effects are predominant, a conclusion arrived at in the discussion of the total-pressure-loss coefficient.

A comparison is given in figure 12 of the diffuser effectiveness obtained if stations III and IV are independently considered the exit of the diffusing bend. The difference between the two curves is the static pressure rise in the downstream duct. It can be seen that this pressure rise increases with increasing inlet boundary layer. For the thinnest inlet-boundary-layer tests, however, the static pressure at the end of the downstream duct was less than the static pressure at the exit of the cascade. For the thickest inlet-boundary-layer tests, this pressure rise amounted to about 40 percent of the over-all static pressure rise. It should be noted, therefore, that a pressure rise can be obtained downstream of the cascade. In this investigation, station III was located just far enough downstream of the airfoils to avoid the separated zone and the discrete wakes from the airfoils.

In the thick boundary-layer range the exit-velocity profile is highly curved. (For example, see fig. 9(b).) When the adverse pressure gradient is small, highly curved profiles tend to revert to the flatter profile characteristic of fully developed turbulent pipe flow. For the same mass flow and mean total pressure, the flatter profile requires a lower mean dynamic pressure and, therefore, a higher static pressure. The pressure rise in the downstream duct is due, therefore, to the flattening of velocity profile. The drop in static pressure for the thinnest inlet boundary layer was due to the friction loss in the downstream duct.

Mach number and airfoil Reynolds number effects.- Figure 13 shows the variation of total-pressure-loss coefficient, diffusion factor, and diffuser effectiveness with mean inlet Mach number and Reynolds number for the thinnest inlet-boundary-layer condition tested. It can be seen that the performance of the cascade is adversely affected by increasing mean inlet Mach number and Reynolds number. Since the mean inlet Mach

number could not be varied without changing the Reynolds number, the two phenomena could not be studied independently. Within the range tested, however, this effect is very small. The same observations hold for the other boundary-layer thicknesses.

General Considerations

No corresponding data for other configurations could be found with which to make a quantitative comparison of the performance of the cascade diffusing bend investigated. The following discussion which holds only for the thick inlet-boundary-layer range is based on the pipe flow data given in reference 5. No comparable data for thin inlet boundary layers could be found. It should be kept in mind that, for the same boundary-layer thickness, the high shape factors used in this investigation would tend to impair the performance of the cascade bend.

If the performance of the cascade bend is compared to a well-designed diffuser or a well-designed diffuser followed by a vaned bend, the pressure recovery of the configuration tested is low and the energy losses are high. For example, for a circular diffuser with an area ratio of 1.45:1 and the optimum expansion angle followed by a 90° turn, the estimated total-pressure-loss coefficient (see reference 5) is about 0.09, which is appreciably less than the value of 0.24 obtained for the diffusing bend. Therefore, when the total-pressure loss is very important and space is available, the cascade diffusing bend is not suitable.

When space and cost considerations limit the length of the configuration, the situation is entirely different. The diffuser-bend combination mentioned previously, for the same size inlet, would be about 65 inches long, whereas the minimum length of the cascade diffusing bend is only about 30 inches. For an area ratio of 2:1, the length of the diffuser-bend combination increases to about 125 inches, whereas the length of the diffusing bend increases to only about 40 inches. It is interesting to note that the cascade diffusing bend investigated had about the same total-pressure-loss coefficient as a vaned bend without any diffusion (reference 5). This result seems to indicate that, when the duct configuration requires a bend, a certain amount of diffusion can be obtained without an appreciable rise in the total-pressure losses.

SUMMARY OF RESULTS

An experimental investigation of a right-angled cascade diffusing bend of area ratio 1.45:1 and a square inlet was conducted in

order to determine the effect on performance of concurrently increasing the boundary-layer thickness and the shape parameter. The results obtained are summarized as follows:

1. For the thick inlet boundary-layer runs:

   (a) The total-pressure losses of the diffusing bend are about equal to the losses of a vaned 90° bend with no diffusion.

   (b) The measured losses of the diffusing bend are larger than those estimated for a circular diffuser of optimum expansion angle with a vaned bend downstream, but the diffusing bend is much shorter.

2. At a mean inlet Mach number of 0.30, the diffuser effectiveness varied from about 0.74 for the tests with the thinnest inlet boundary layer to about 0.19 for the tests with thickest inlet boundary layer. The total-pressure-loss coefficient for the tests with the thinnest inlet boundary layer was about 0.11 and increased to about 0.24 for the thickest inlet boundary layers.

3. The results indicate that the airfoil profile losses are only a small part of the total losses and that the boundary-layer effects are predominant. It would seem likely, therefore, that a large improvement in performance could be obtained through the use of boundary-layer control.

4. Investigation of the effect of inlet Mach number shows that the performance of the cascade is adversely affected by an increase in the mean inlet Mach number and Reynolds number. Within the range tested, however, this effect is small.

5. Except when the inlet boundary layer was very thin, the static pressure at the exit of the constant-area duct downstream of the bend was higher than at a station immediately downstream of the cascade of airfoils. This increase was due to the flattening of the velocity profile as the air flowed down the duct.

Langley Aeronautical Laboratory
National Advisory Committee for Aeronautics
Langley Field, Va., December 13, 1951

REFERENCES

1. Erwin, John R., and Emery, James C.: Effect of Tunnel Configuration and Testing Technique on Cascade Performance. NACA Rep. 1016, 1951. (Supersedes NACA TN 1016.)

2. Kantrowitz, Arthur, and Erwin, John R.: Cascade Investigation of Buckets for a Modern Aircraft Turbosupercharger. NACA ACR L4J25, 1944.

3. Westphal, Willard R., and Dunavant, James C.: Application of Wire-Mesh Plotting Device to Incompressible Cascade Flows. NACA TN 2095, 1950.

4. Tetervin, Neal: A Review of Boundary-Layer Literature. NACA TN 1384, 1947.

5. Henry, John R.: Design of Power-Plant Installations. Pressure-Loss Characteristics of Duct Components. NACA ARR L4F26, 1944.

TABLE I

BOUNDARY-LAYER SCREEN AND FENCE DATA

Configuration	Fence projection (in.)	5-foot duct	Screens		
			Mesh per inch	Wire diam. (in.)	Hole size (in.)
1	0	Removed	-------	-----	-------
2	0	In	-------	-----	-------
3	0	In	16 × 16	0.010	15 × 15
4	1	In	40 × 40	.009	16 × 16
			16 × 16	.010	10 × 10
5	2	In	80 × 80	.006	13 × 13
			16 × 16	.010	7 × 7

NACA

TABLE II

BOUNDARY-LAYER PARAMETERS

Configuration	1	2	3	4	5
Inlet data					
Two-dimensional at center of wall					
δ^*	0.033	0.17	0.40	1.34	2.12
θ	.027	.14	.30	.92	1.27
H	1.22	1.22	1.34	1.45	1.67
δ	.21	1.21	2.28	5.38	6.63
Two-dimensional in corners[1]					
δ^*	0.125	0.45	1.06	4.05	5.30
θ	.089	.33	.67	1.66	1.87
H	1.42	1.38	1.58	2.44	2.84
δ	.55	2.28	3.67	8.45	10.67
Three dimensional					
Δ^*	2.48	13.6	30.7	104.7	148.8
ϕ	2.07	10.3	22.7	57.9	71.1
$\overline{H}$	1.22	1.32	1.35	1.81	2.09
Three-dimensional exit data					
Δ^*	25.0	68.4	115.4	242.3	282.7
ϕ	22.6	47.7	66.3	97.0	104.8
$\overline{H}$	1.11	1.44	1.73	2.50	2.70

[1]Measured in a plane located at the intersection of the two walls and forming an angle of 45° with either wall.

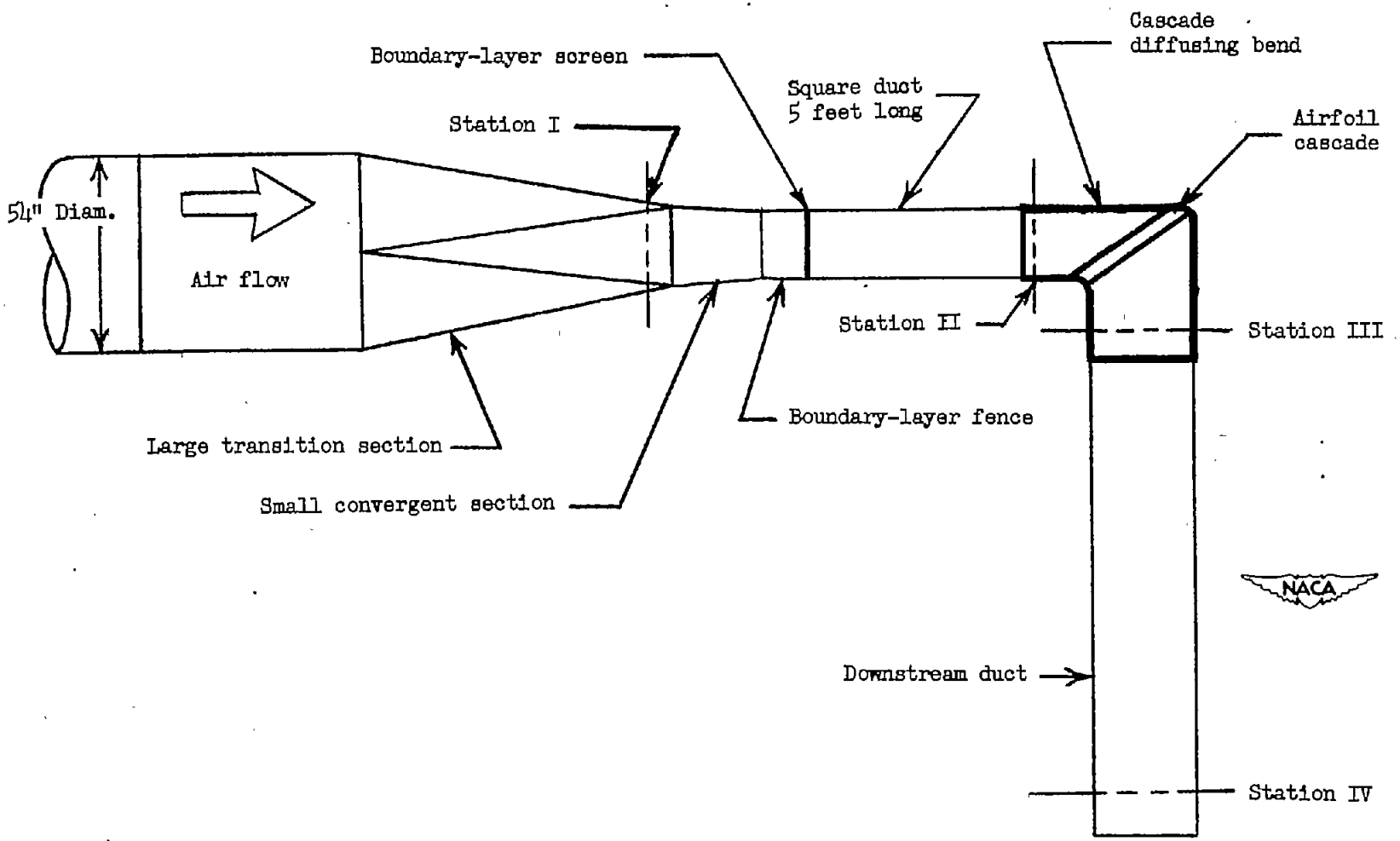

Figure 1.- Schematic sketch of the experimental setup.

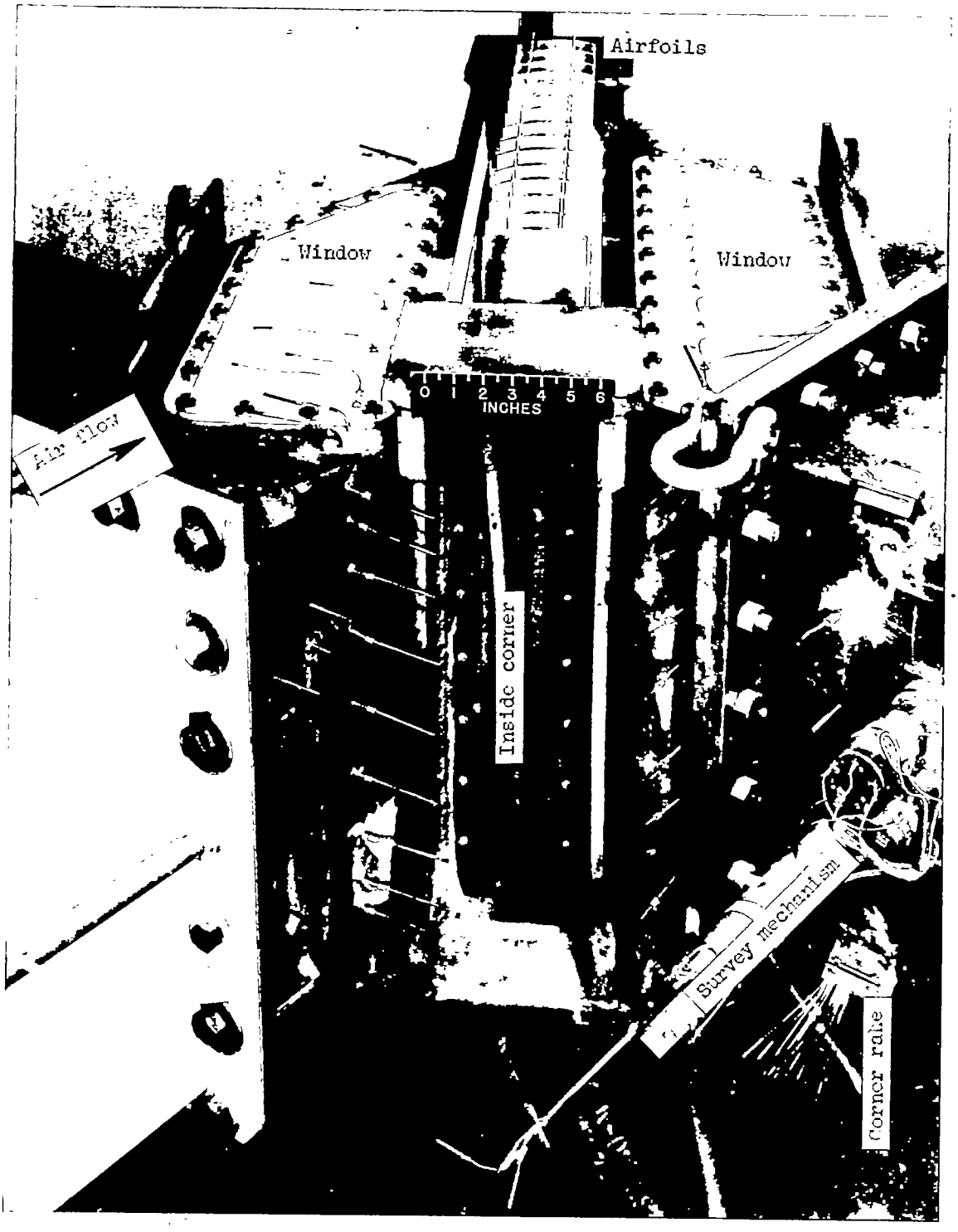

Figure 2.- Cascade-type diffusing bend.

L-65680.1

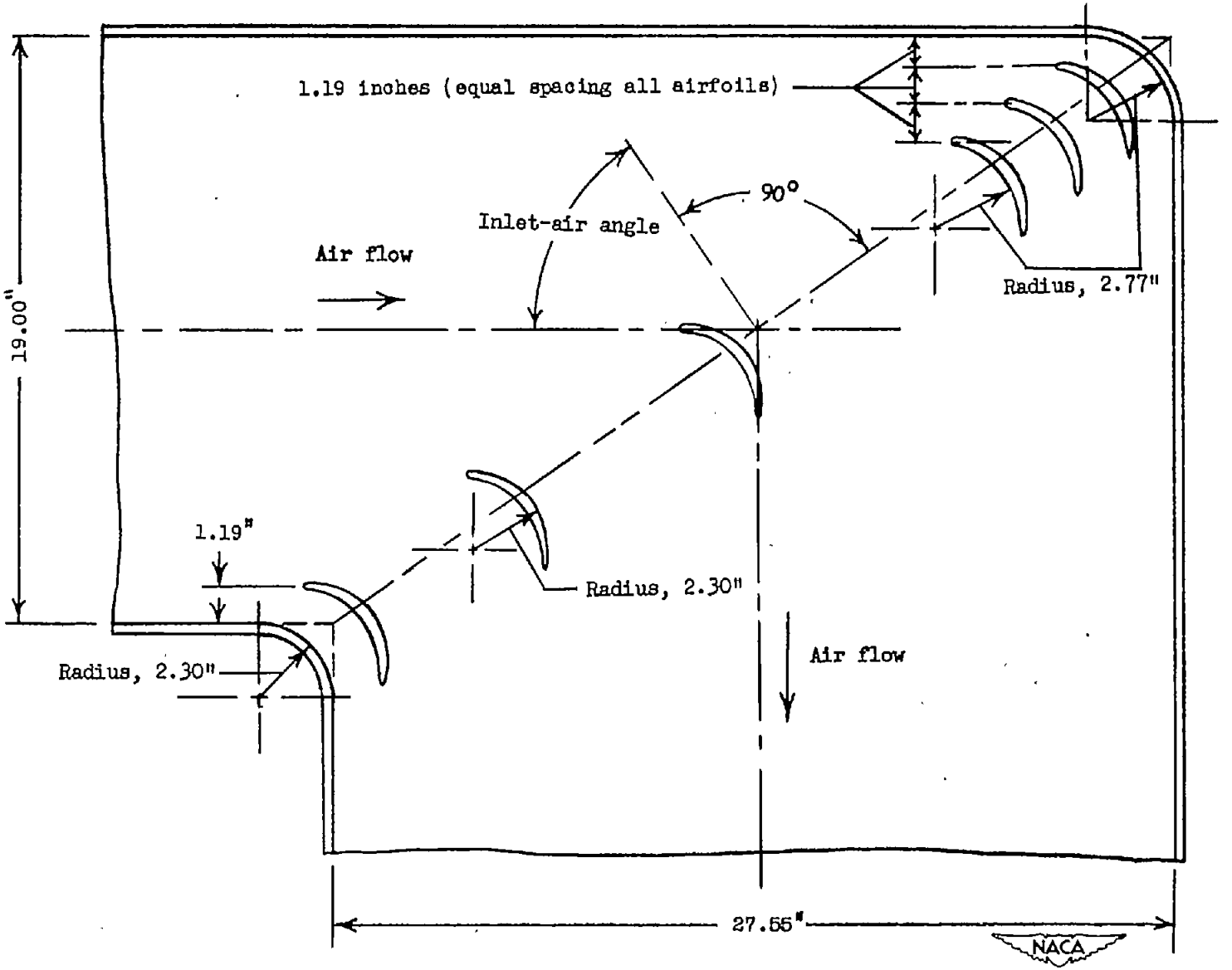

Figure 3.- Sketch showing airfoil location and cascade end condition.

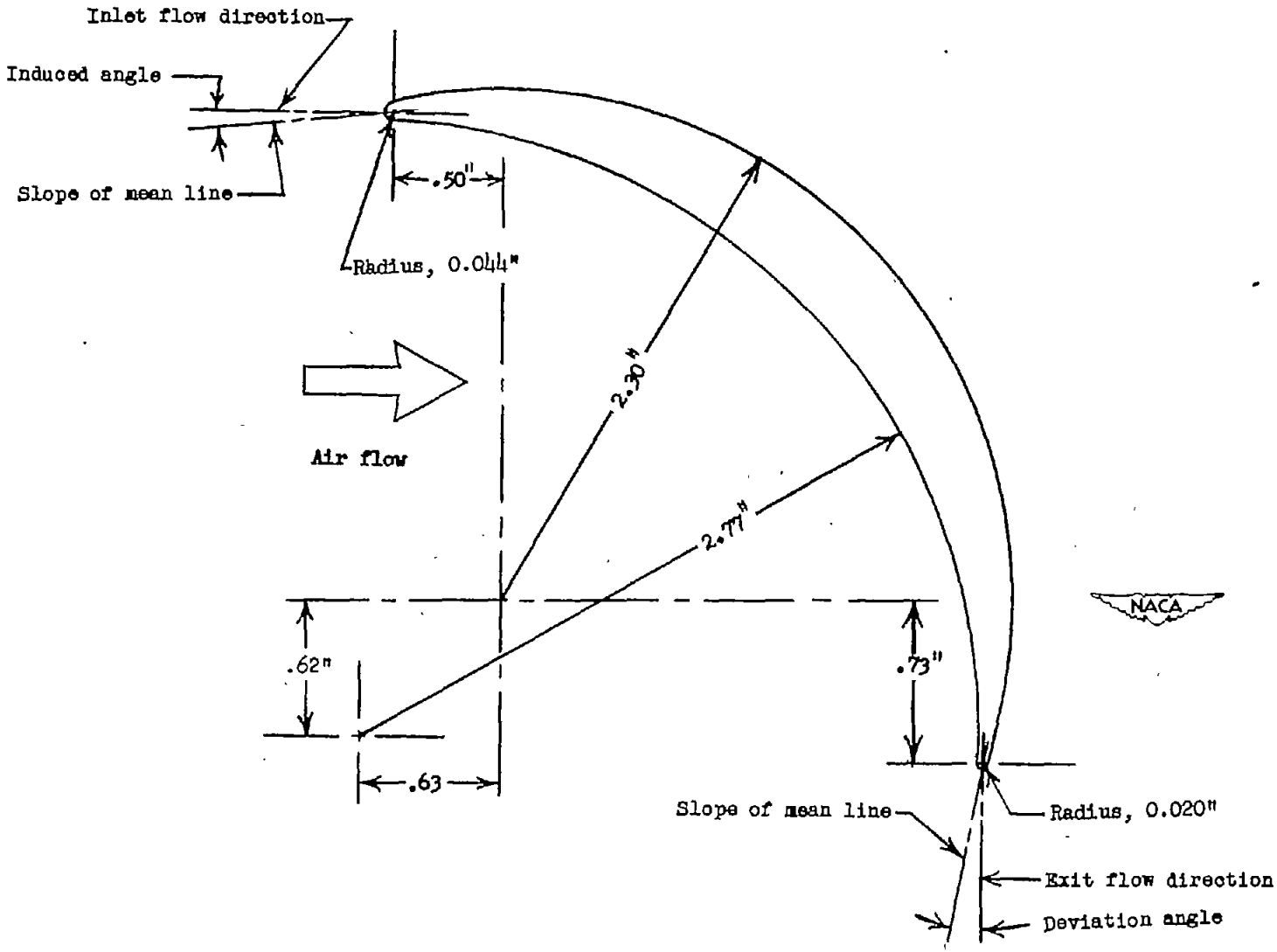

Figure 4.- Airfoil profile.

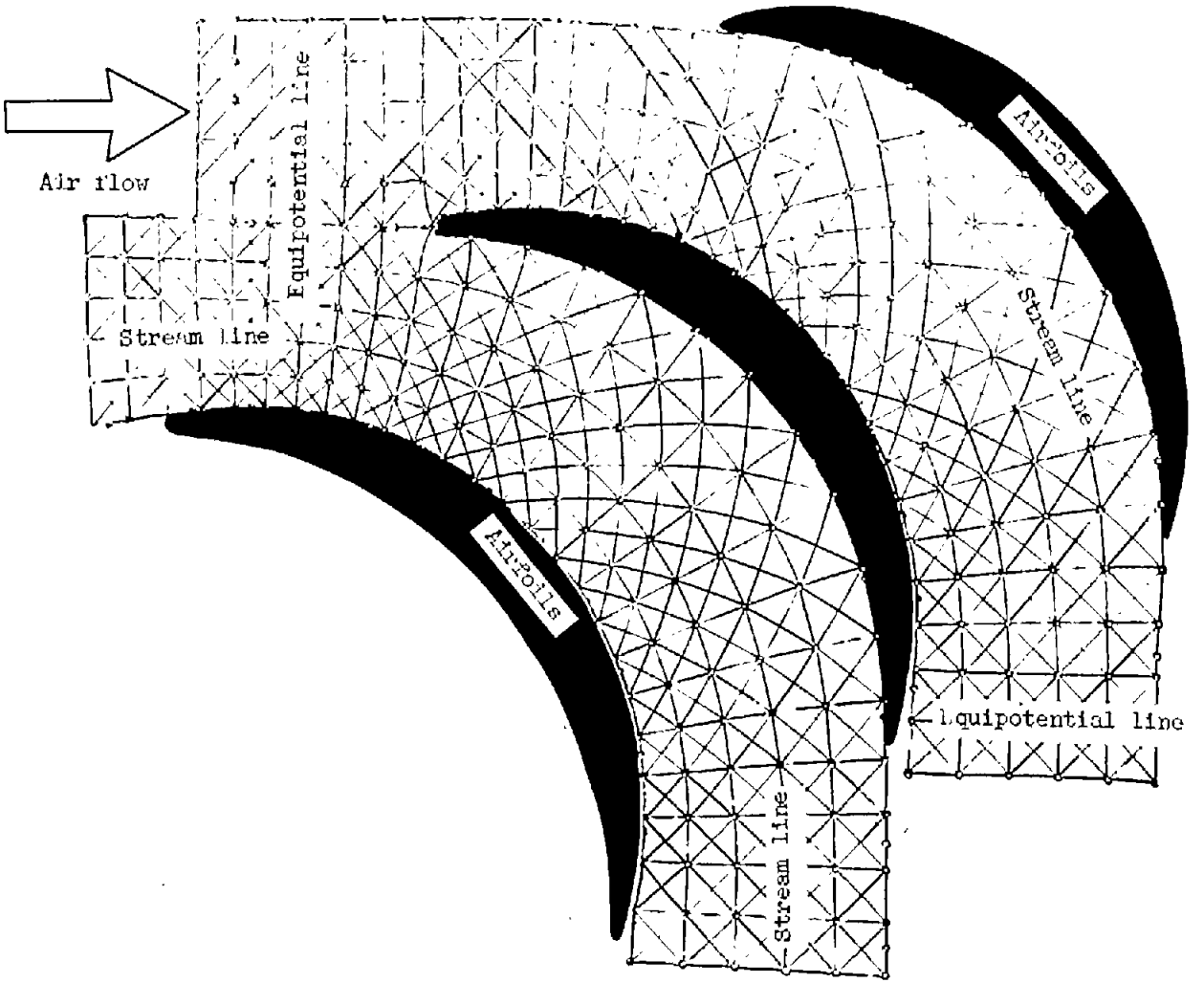

Figure 5.- Photograph of flow-pattern plotting device.

NACA

L-65474.1

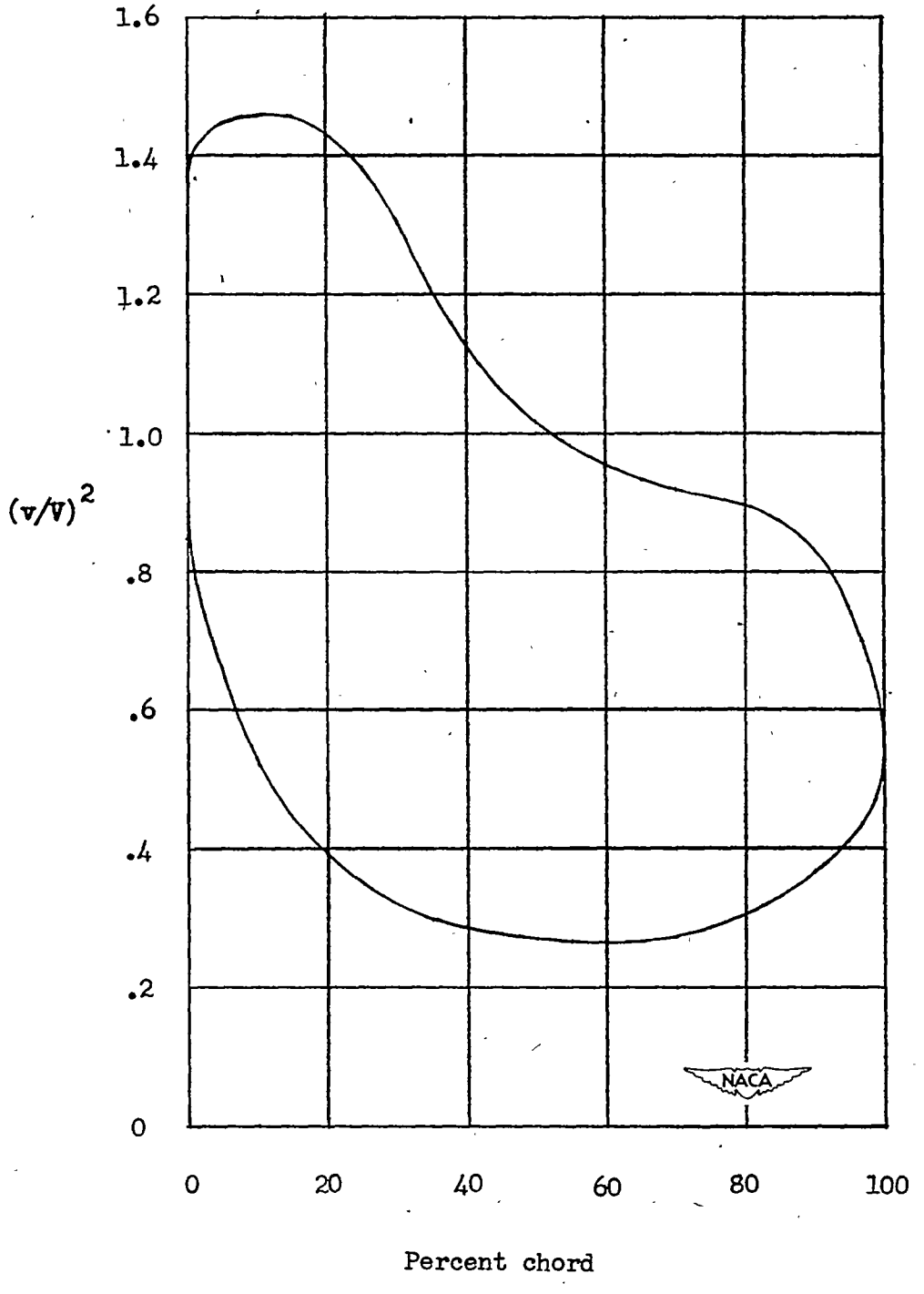

Figure 6.- Theoretical pressure distribution on airfoil in cascade.

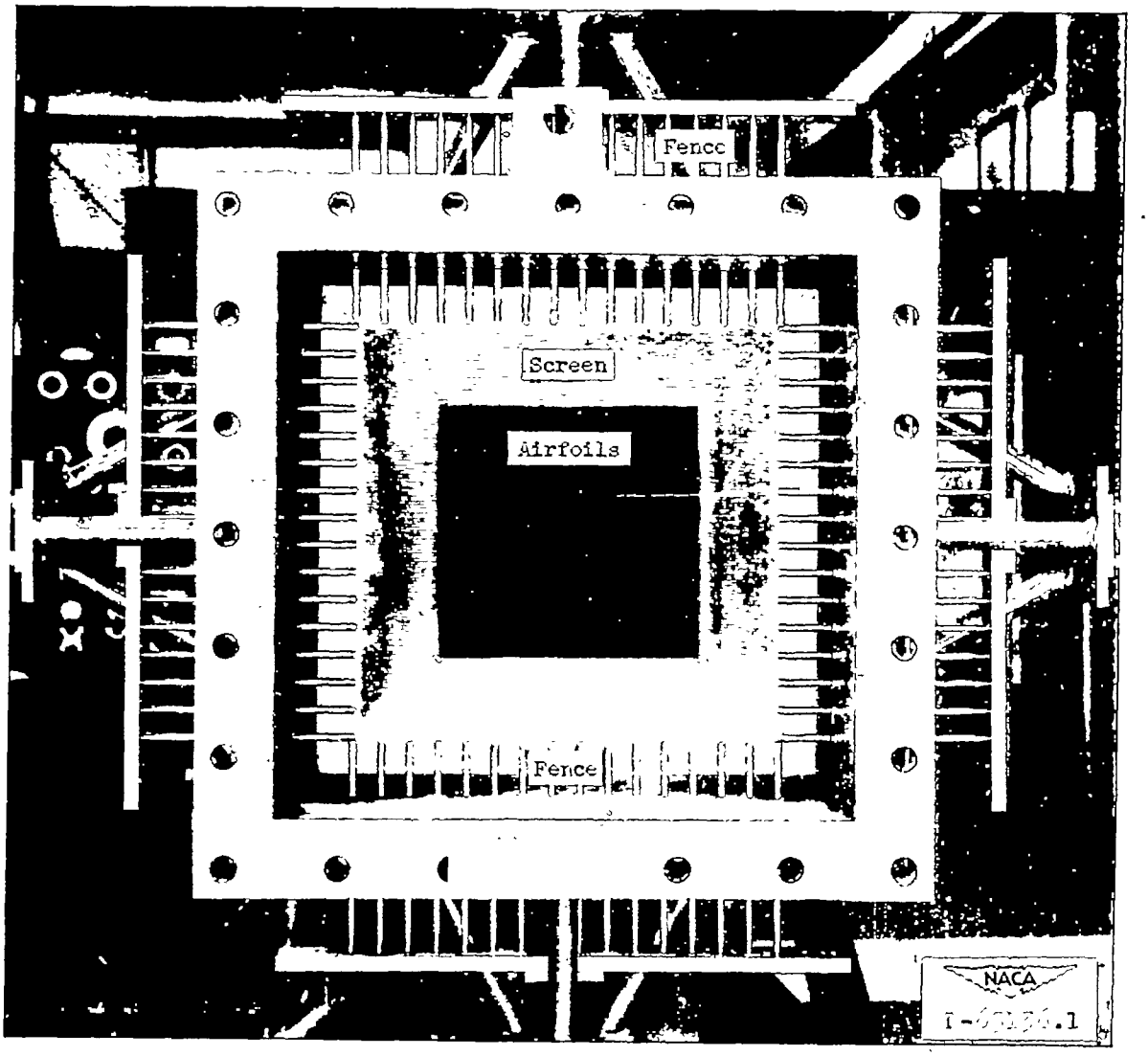

Figure 7.- Boundary-layer screens and fence setting for the thickest inlet boundary layer (configuration 5).

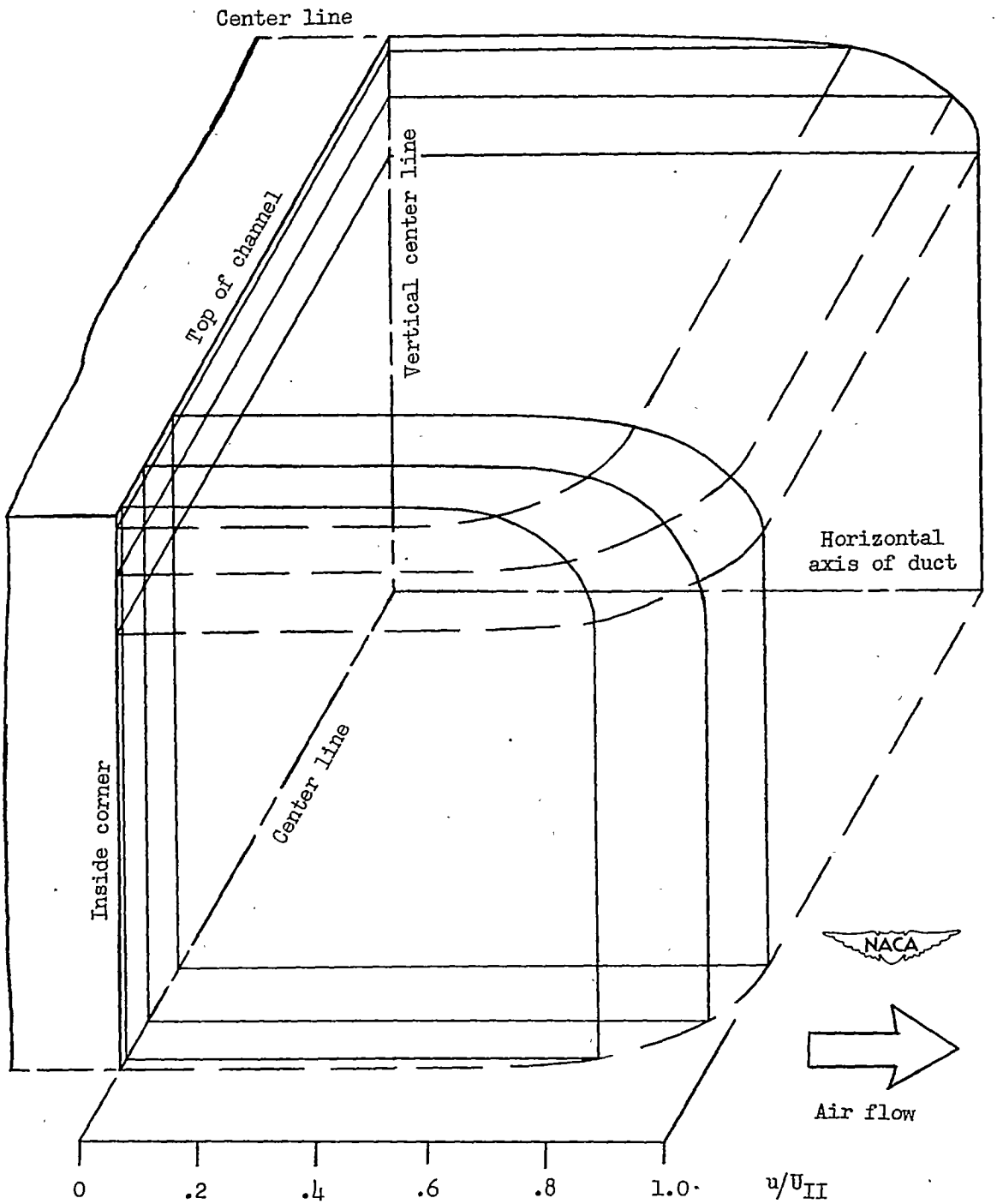

(a) Inlet station preceded by 5-foot duct (configuration 2).

Figure 8.- Inlet-velocity distribution (station II).

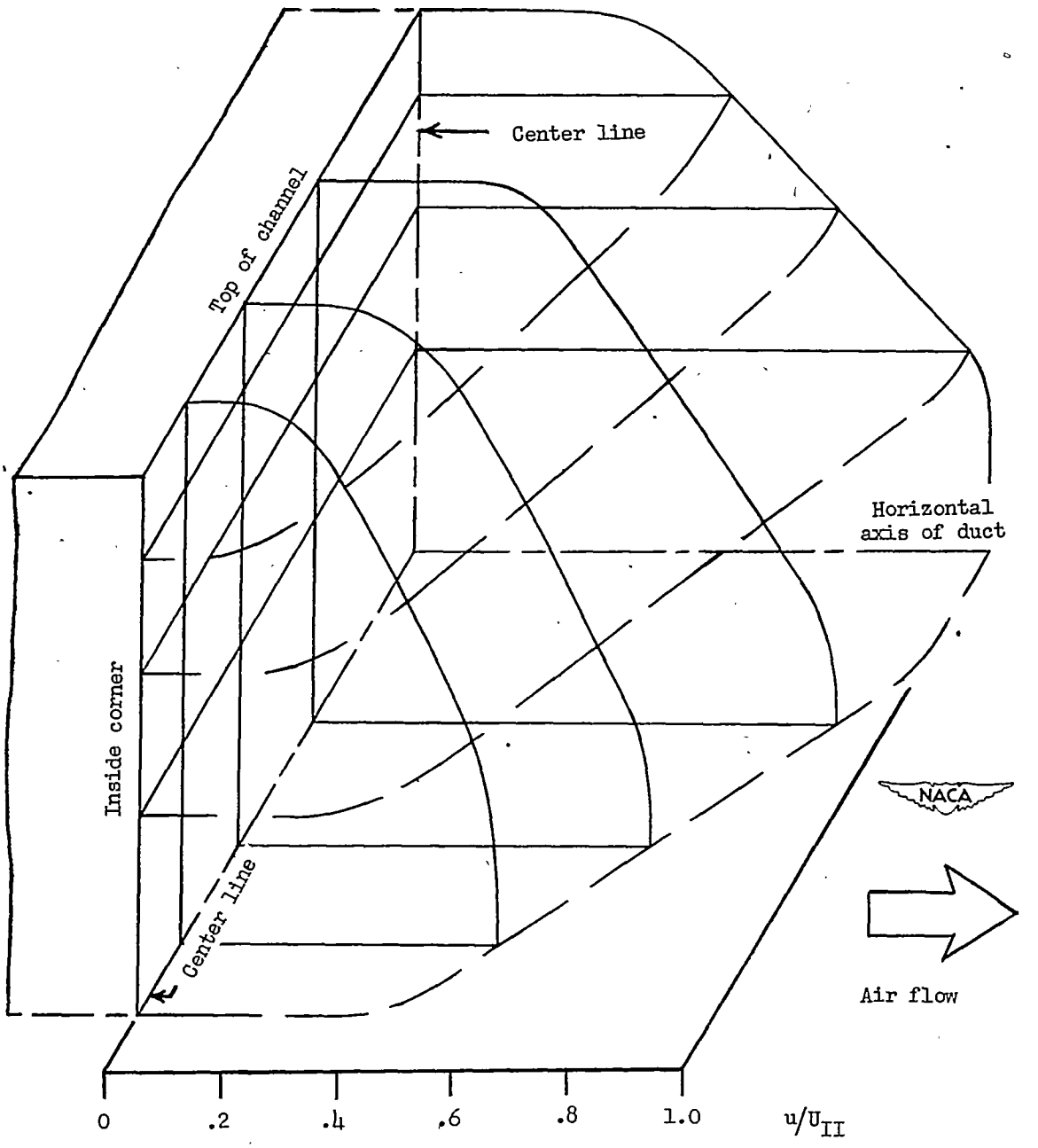

(b) Thickest inlet boundary layer (configuration 5).

Figure 8.- Concluded.

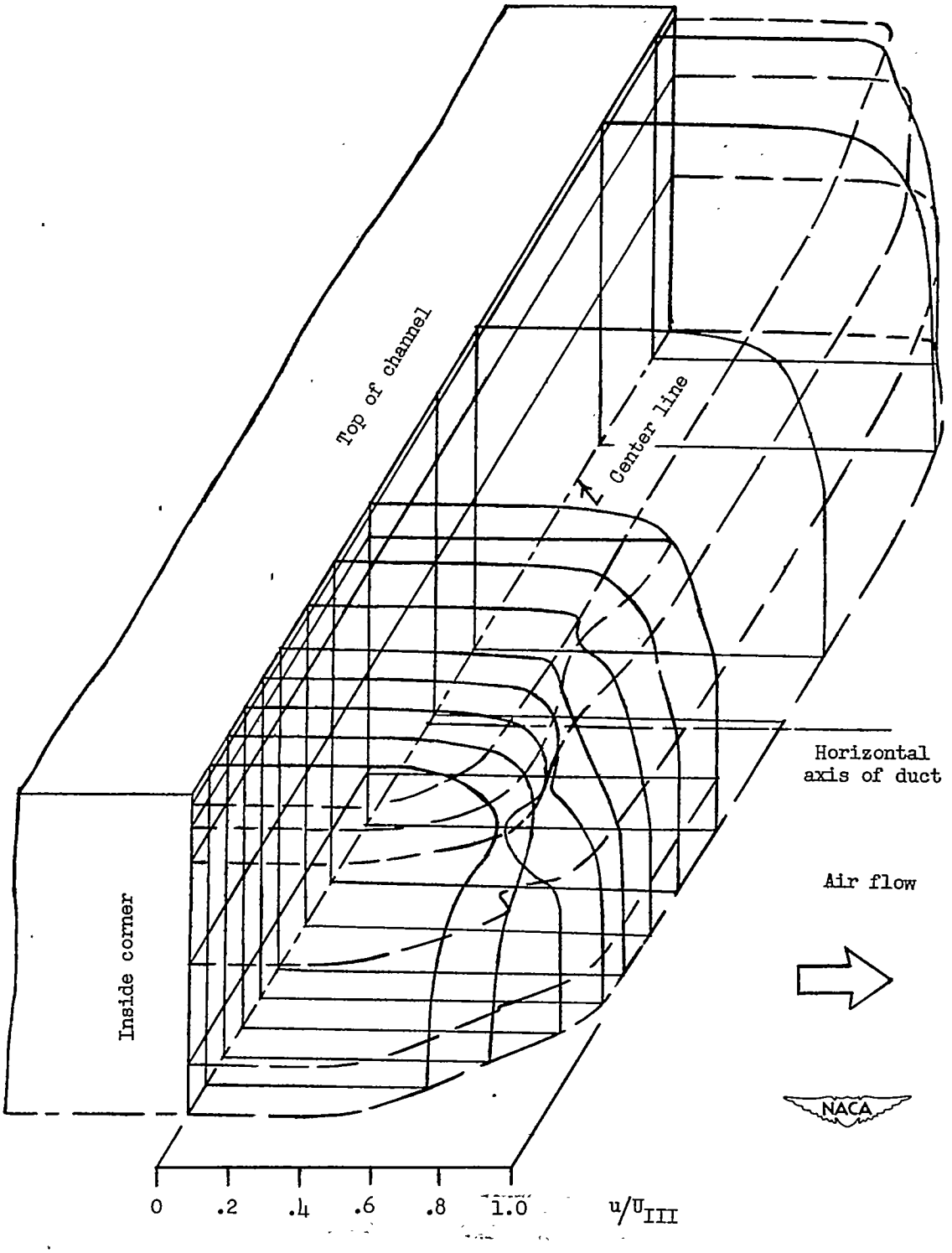

(a) Inlet station preceded by 5-foot duct (configuration 2).

Figure 9.- Exit velocity distribution (station III).

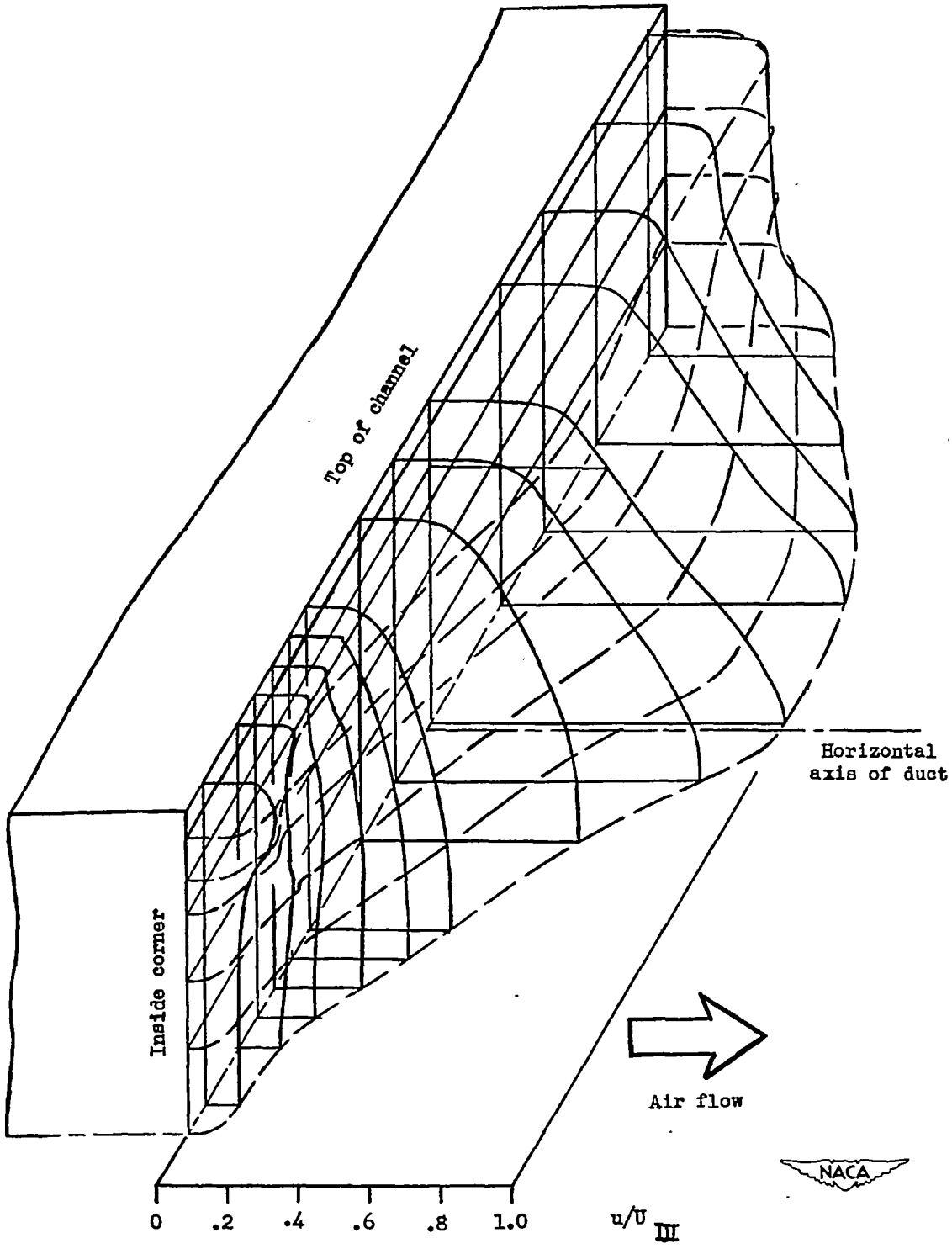

(b) Thickest inlet boundary layer (configuration 5).

Figure 9.- Concluded.

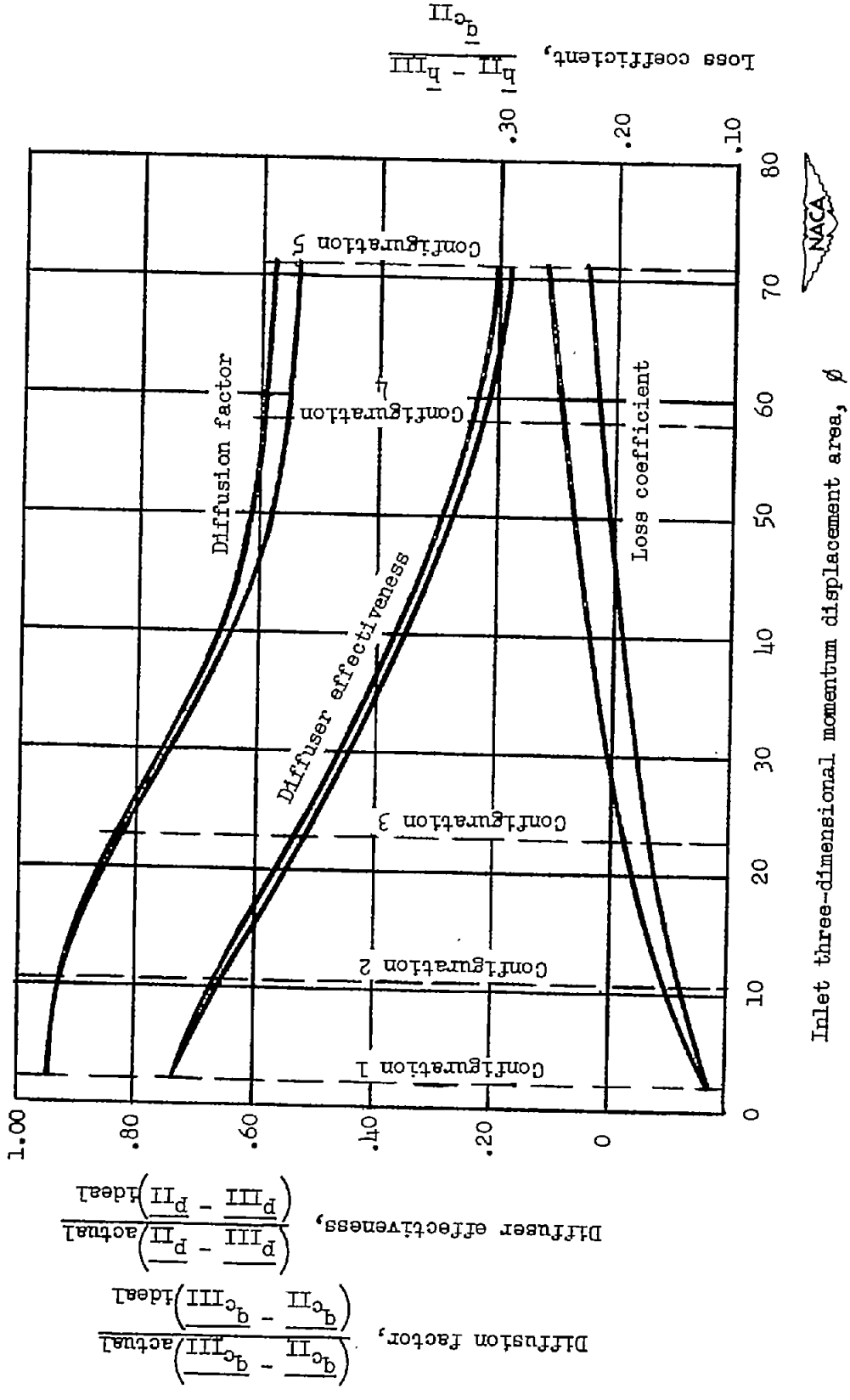

Inlet three-dimensional momentum displacement area, ϕ

Figure 10.- Variation of performance parameters with inlet momentum area at a mean inlet Mach number of 0.30.

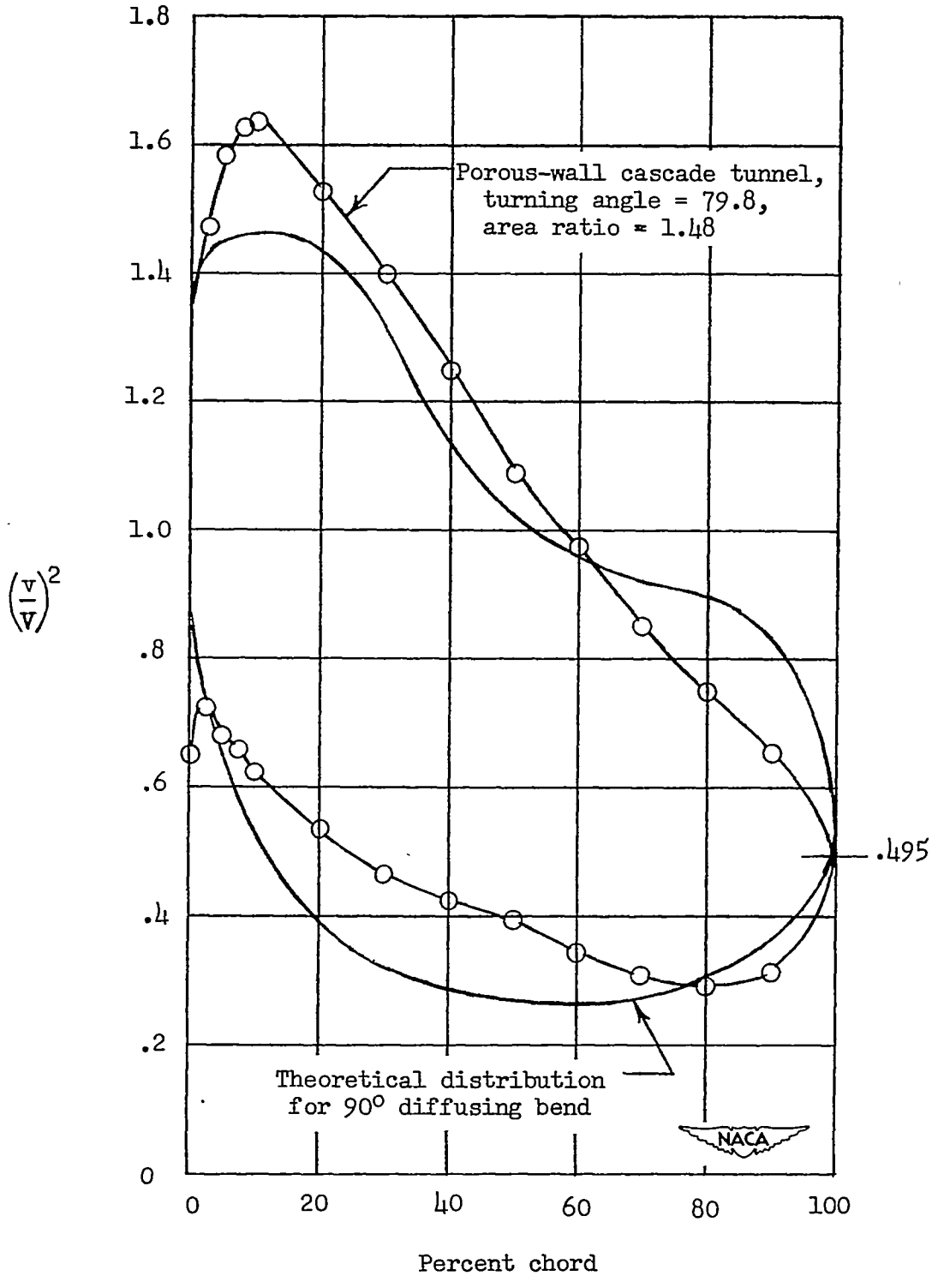

Figure 11.- Pressure distribution on airfoil in cascade.

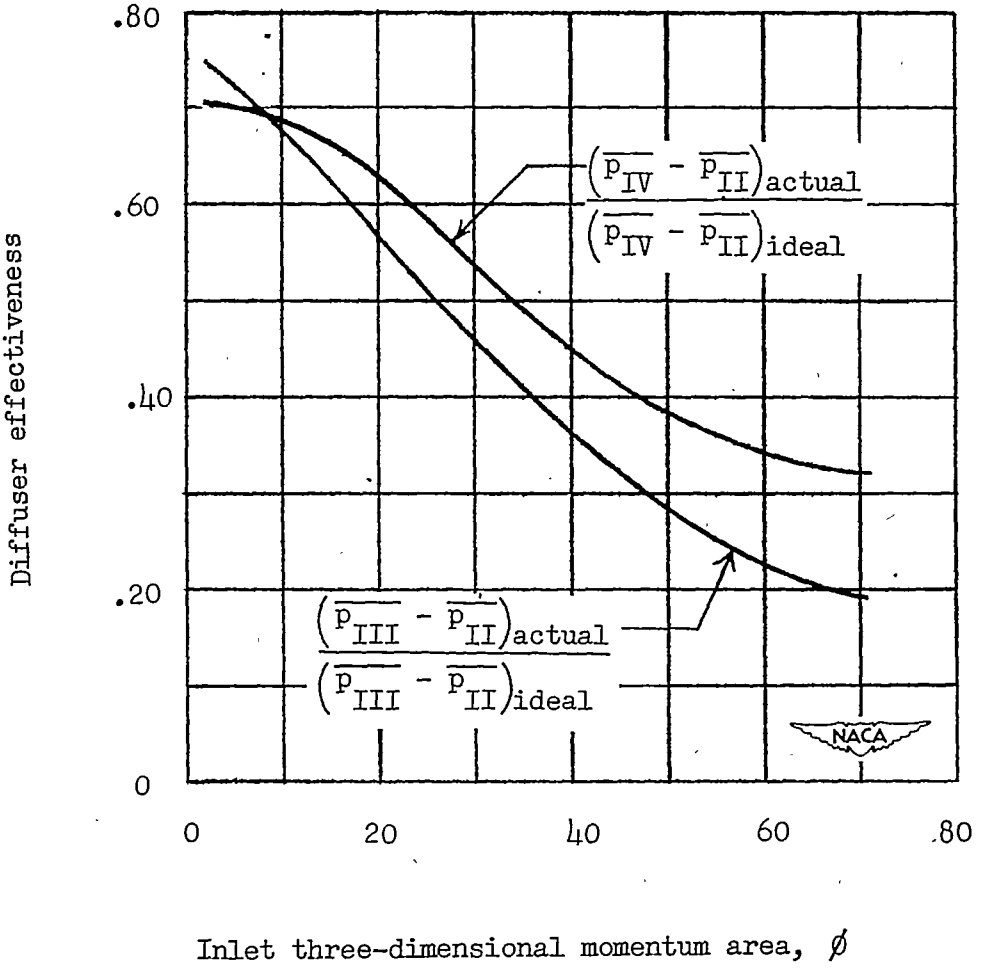

Figure 12.- Variation of diffuser effectiveness with inlet momentum area for two different exit stations.

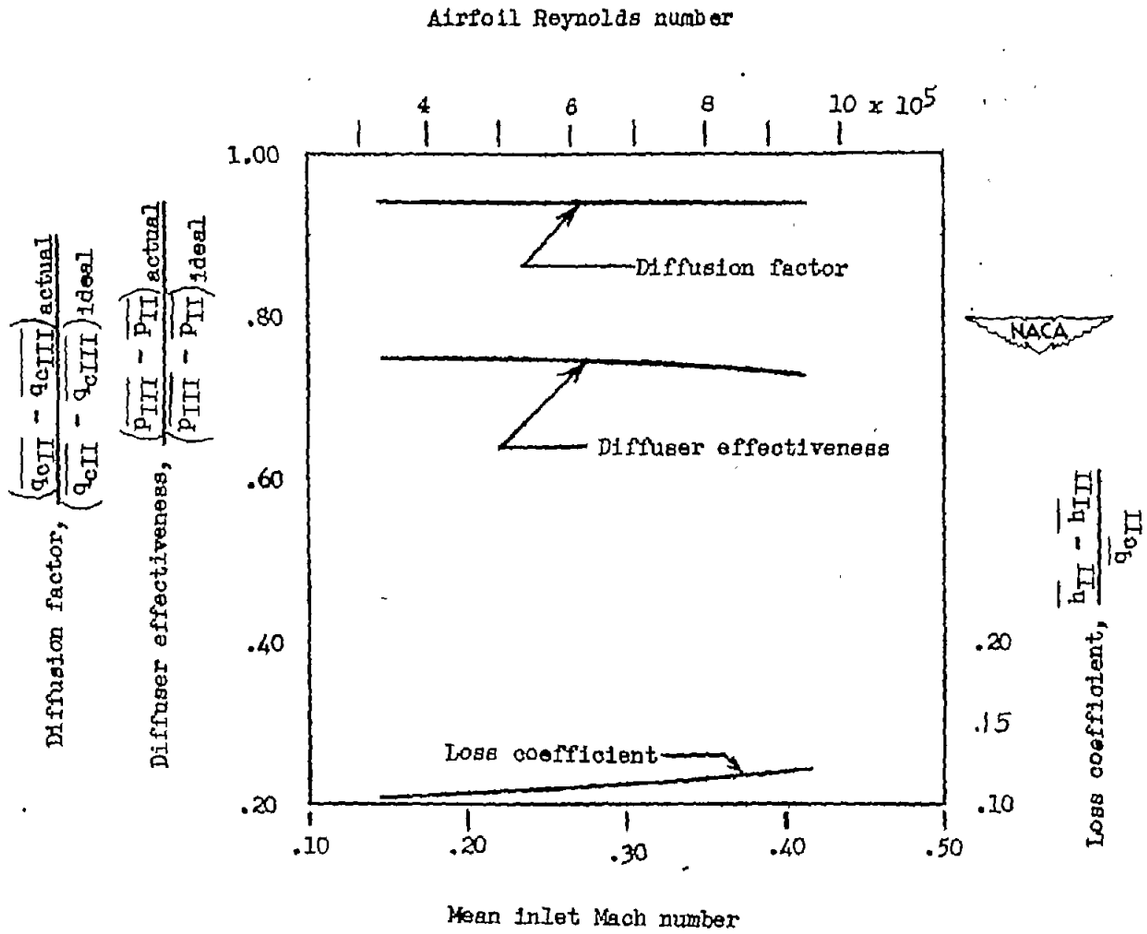

Figure 13.- Variation of performance parameters with mean inlet Mach number and airfoil Reynolds number for the thinnest inlet boundary layer (configuration 1).

NACA-Langley - 4-8-53 - 1000